Cytometry 12:479–485 (1991)

OPTICAL TRAPPING

Experimental and Theoretical Investigations on the Validity of the Geometrical Optics Model for Calculating the Stability of Optical Traps

Tom C. Bakker Schut, Gerlo Hesselink, Bart G. de Grooth, and Jan Greve
Department of Applied Physics, Cell Characterization Group, University of Twente, The Netherlands

Received for publication July 7, 1990; accepted March 12, 1991

We have developed a computer program based on the geometrical optics approach proposed by Roosen to calculate the forces on dielectric spheres in focused laser beams. We have explicitly taken into account the polarization of the laser light and thd divergence of the laser beam. The model can be used to evaluate the stability of optical traps in a variety of different optical configurations.

Our calculations explain the experimental observation by Ashkin that a stable single-beam optical trap, without the help of the gravitation force, can be obtained with a strongly divergent laser beam. Our calculations also predict a different trap stability in the directions orthogonal and parallel to the polarization direction of the incident light.

Different experimental methods were used to test the predictions of the model for the gravity trap. A new method for measuring the radiation force along the beam axis in both the stable and instable regions is presented. Measurements of the radiation force on polystyrene spheres with diameters of 7.5 and 32 μm in a TEM_{00}-mode laser beam showed a good *qualitative* correlation with the predictions and a slight *quantitative* difference.

The validity of the geometrical approximations involved in the model will be discussed for spheres of different sizes and refractive indices.

Key terms: Radiation pressure calculations, radiation pressure measurements, influence of polarization on radiation pressure

According to Maxwell, an electromagnetic wave carries a certain momentum which causes a pressure that is equal to the energy density of the wave. Because momentum is conserved light that is scattered will exert a force on the scattering object.

This phenomenon, known as radiation pressure, can be used to levitate small particles, such as cells and cellular parts, as first shown experimentally by Ashkin (1). Using one or more focused laser beams one can build stable optical traps which can be used as tools for micro manipulation of cells, parts of cells, bacteria, viruses, etc. (1,4,6,8).

In order to use radiation pressure as a quantitative tool to measure the forces occurring at cell-cell adhesion, cell-surface adhesion, cell-antibody binding, or even forces inside cells for example during cell division, one must know the magnitude and direction of the forces exerted by the light.

Using the geometrical optics model for calculating the radiation pressure on dielectric spheres, developed by Roosen (12), one can calculate in a relatively simple way the magnitude and direction of the force that is exerted by a divergent laser beam on a dielectric sphere. This model is only valid for spheres that are large as compared to the wavelength. Cells and cellular parts, however, barely fulfill this criterion and therefore using the model to calculate the forces *on these* objects is questionable.

In order to study the validity of the geometrical optics model to predict the magnitude and direction of the

optical forces and the stability of optical traps we have developed a computer program, based on the calculations of Roosen (12), which explicitly takes the polarization and the divergence of the laser beam into account.

We have calculated the forces exerted by the laser light during optical trapping in a variety of different optical configurations. These configurations include different polarization directions of the incoming light and the experimental conditions for the single beam gradient force optical trap as realized experimentally by Ashkin (5).

In order to test the predictions of the model for spheres inside a gravity trap we have measured the radiation forces on dielectric spheres (with diameters of 7.5 and 32 μm) in water. A new dynamic method has been developed to measure the force along the beam axis in both the stable and instable regions.

FORCE CALCULATIONS

According to Maxwell the radiation pressure P of a plane electromagnetic wave in vacuum equals the energy density of the wave and has the direction of the propagation of the light:

$$P = \frac{E^2}{2\,\mu_0 \cdot c^2}, \tag{1}$$

where E is the electric field strength, μ_0 is the vacuum permeability, and c is the velocity of light. If we consider particles that are large compared to the wavelength, i.e., $2\pi\rho/\lambda \geq 100$, where ρ is the radius of the particle and λ is the wavelength of the electromagnetic wave, the processes of reflection, refraction, and diffraction may be considered as independent and the resulting forces can be added (9). In the case of large spheres, diffraction effects are of second order and can be neglected (9).

The force F on a total absorbing surface S, with an angle *i* between the direction of light propagation and the normal on the surface, is then given by

$$F = \frac{S \cdot E^2 \cdot \cos i}{2\,\mu_0 \cdot c^2}. \tag{2}$$

If a part of the incoming light is reflected and a part is transmitted, we can describe this process as total asborption followed by emission of a part of the light in the direction of reflection and a part in the direction of transmission.

The resulting force on the scattering surface is a result of these three forces:

$$\vec{F} = \vec{F}_{abs} + \vec{F}_{refl} + \vec{F}_{trans}. \tag{3}$$

In the geometrical optics approach we can calculate the force f_z that one ray exerts on a surface element ∂S (the ray is defined as the light that hits ∂S) and then integrate over all rays that hit the surface of the sphere. If we consider a isotropic nonabsorbing sphere with refractive index n_s and radius r in a surrounding

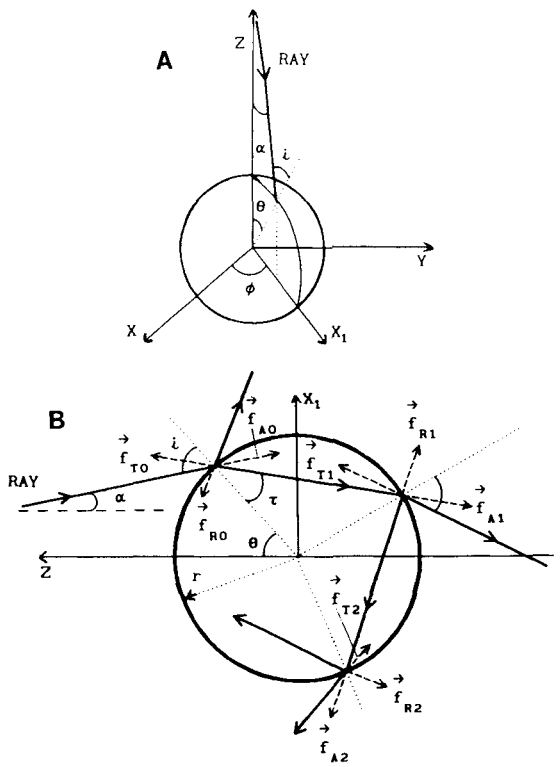

FIG. 1. **A:** Definition of axes and angles: *i* is the angle of incidence, α is the angle between the z axis and the ray, θ and φ are spherical coordinates, X, Y and Z are normal Cartesian coordinates, X_1 is a transformed axis that lies in the plane of reflection. **B:** Absorption, reflection, and refraction of a light ray that hits a sphere with radius r; the refractive index of the sphere is larger than the refractive index of the surrounding medium. The angle of incidence $i = \theta + \alpha$ and the angle of refraction is τ. f_{A_i} is the force caused by total absorption at transition i, f_{T_i} is the force caused by partial transmission at transition i, and f_{R_i} is the force caused by partial reflection at transition i.

medium with refractive index n_m ($n_s > n_m$), we can write for the force f_z in the direction of z (see Fig. 1):

$$f_z = \partial F_z / \partial S = \sum_{i=0}^{\infty} f_{z_{Ai}} + f_{z_{Ti}} + f_{z_{Ri}}, \tag{4}$$

where $f_{z_{Ai}}$ is the force in the direction of z caused by absorption at transition i, $f_{z_{Ti}}$ is the force in the direction of z caused by transmission at transition i, and $f_{z_{Ri}}$ is the force in the direction of z caused by reflection at transition i. For a nonabsorbing medium the following relations must hold:

$$f_{zT0} + f_{zA1} = 0$$

and

$$f_{zR(i+1)} + f_{zA(i+2)} = 0.$$

Therefore the force F_z is given by

$$f_z = f_{z_{A0}} + f_{z_{R0}} + \sum_{i=0}^{\infty} f_{z_{T(i+1)}}. \tag{5}$$

$f_{z_{A0}}$ can be calculated using Eq. 2; in a medium with refractive index n_m the speed of light c must be replaced by $v = c/n_m$ (7) so that $f_{z_{A0}}$ is given by

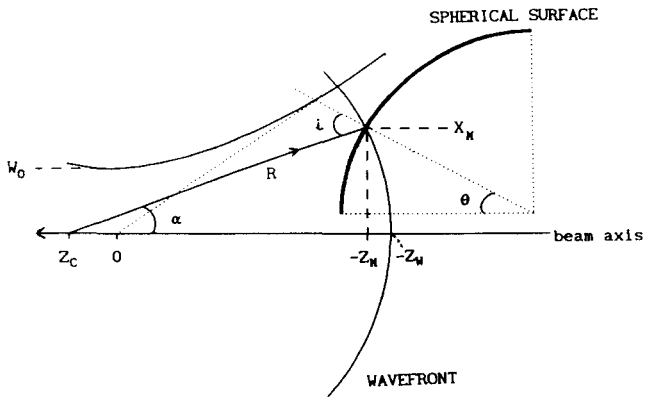

FIG. 2. Determination of the angle α between the beam axis and the ray of a gaussian laser beam that hits the point $M(X_m,Z_m)$ of a spherical surface. R is the radius of the spherical wave front, Z_C is the point from which the ray seems to come, assuming that the ray is orthogonal to the wave front, and w_0 is the beam waist at the focus (at z = 0).

$$f_{z_{A0}} = -\frac{n_m^2 \cdot E^2 \cdot \cos i}{2\,\mu_0 \cdot c^2} \cdot \cos(i-\theta) = -C \cdot \cos(i-\theta). \tag{6}$$

$f_{z_{R0}}$ is given by

$$f_{zR0} = -R \cdot C \cdot \cos(i+\theta). \tag{7}$$

$f_{z_{T(i+1)}}$ is given by

$$f_{zT(i+1)} = C \cdot T^2 \cdot R^i \cdot \cos[(i+\theta-2\tau) + i\cdot(\pi-2\tau)],$$

and

$$\sum_{i=0}^{\infty} f_{z_{T(i+1)}} = C \cdot \frac{T^2 \cdot [\cos(i+\theta-2\tau) + R \cdot \cos(i+\theta)]}{1 + R^2 + 2R \cdot \cos 2\tau}. \tag{8}$$

R and T are the fresnel coefficients for reflection and transmission (dependant of the polarization of the incoming light and the angle on incidence).

Equation 5 yields f_z =

$$-C\left(\cos(i-\theta) + R \cdot \cos(i+\theta) - \frac{T^2 \cdot [\cos(i+\theta-2\tau) + R \cdot \cos(i+\theta)]}{1 + R^2 + 2R \cdot \cos 2\tau}\right). \tag{9}$$

Using Eq. 6 and integrating over the surface of the sphere using spherical coordinates, yields

$$F_z = \int_0^{\pi/2} d\theta \int_0^{2\pi} d\phi \cdot f_z \cdot r^2 \cdot \sin\theta =$$
$$-\int_0^{\pi/2} d\theta \int_0^{2\pi} d\phi \frac{E^2 \cdot \cos i \cdot r^2 \cdot \sin\theta \cdot n_m^2}{2\mu_0 c^2}$$
$$\times\left(\cos(i-\theta) + R \cdot \cos(i+\theta) - \frac{T^2 \cdot [\cos(i+\theta-2\tau) + R \cdot \cos(i+\theta)]}{1 + R^2 + 2R \cdot \cos 2\tau}\right). \tag{10}$$

Similar expressions can be found for the X and Y direction.

The angle of incidence of the ray can be determined using the geometrical optics representation of laser beams (11). The wave front is considered spherical and its radius of curvature R varies with the distance from the beam waist (see Fig. 2). For every point $(M(X_M,Z_M)$ on the surface of the sphere that is hit by a ray one can calculate the position Z_C from which the ray seems to come, the angle α between the ray and the beam axis, and the intensity of the beam in $M(X_M,Z_M)$. The intensity is given by

$$E^2(X_M, Z_M) = E_0^2 \exp\left(\frac{-2\,X_M^2}{w(Z_M)^2}\right) \tag{11}$$

with

$$w(Z_M) = w_0 \cdot \sqrt{1 + \left(\frac{\lambda \cdot Z_M}{\pi \cdot w_0^2}\right)^2} \quad \text{(radius of the beam)}. \tag{12}$$

The flux Φ of the laser beam is given by

$$\Phi = \int\int_{-\infty}^{\infty} \frac{E^2 \cdot n_m}{2\,\mu_0 \cdot c} ds \tag{13}$$

and therefore

$$E_0^2 = \frac{4\,\Phi \cdot \mu_0 \cdot c}{w_0^2 \cdot \pi \cdot n_m}. \tag{14}$$

The radius of curvature R is given by

$$R(z) = z\left[1 + \left(\frac{\pi w_0^2}{\lambda z}\right)^2\right]. \tag{15}$$

The angle of incidence i for a given value of Φ can be calculated by (see Fig. 1); then $i = \alpha + \theta$. One finds that X_M is given by (see Fig. 2)

$$X_M^2 = R^2(X_W) - [R(Z_W) - (Z_W - Z_M)]^2. \tag{16}$$

From this equation the value of Z_W for a given X_M and Z_M can be calculated. One finds

$$Z_C = R(Z_W) - Z_W \tag{17}$$

and

$$\sin\alpha = \frac{X_M}{R(Z_W)}. \tag{18}$$

The total force exerted by the beam on the sphere can be obtained by calculating the forces for each value of ϕ, transforming back to the original XYZ coordinates and integrating over the surface of the sphere using Eq. 10.

NUMERICAL RESULTS

Using the geometrical optics approach we developed a program to calculate the forces exerted by a divergent beam on dielectric particles of different refractive index and size. The program was written in Pascal and can be run on any MS DOS personal computer. In short the program works as follows. There are six independent parameters, i.e., wavelength, radius of the beam waist, radius of the sphere, relative refractive index of the sphere, distance between the center of the sphere and the beam axis, and the distance between the center of the sphere and the beam waist. Of these six parameters one parameter can be made variable over a certain (adjustable) range and then F_Z and F_Y are calculated for an (adjustable) number of values in the given range using the following procedure. For a given value of ϕ, Eq. 9 is calculated (using the coordinate transformation which puts the X axis in the plane of reflection) for a number of values of θ (using Eqs. 11–18 and the

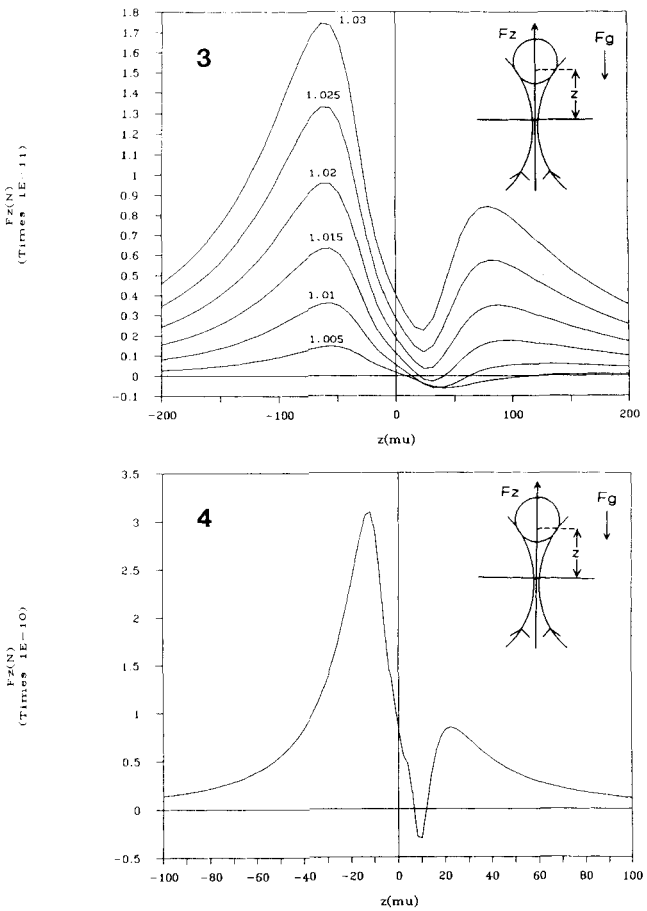

FIG. 3. Calculated values of the radiation force f(z) on a sphere as a function of z for different relative refractive indices; radius of the sphere = 3.75 μm and radius of the beam waist at the focus = 1.8 μm.

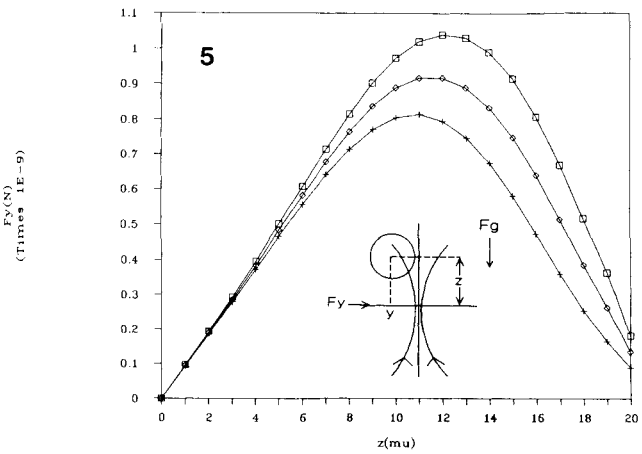

FIG. 4. F(z) as a function of z for a glass sphere in a strongly divergent laser beam; radius of th sphere = 5.0 μm and radius of the beam waist at the focus = 0.29 μm.

FIG. 5. F(y) as a function of y for a sphere in vacuum using different polarizations of the incident light; radius of the sphere = 20 μm and the refractive index = 1.5; the beam is cylindric with a radius of 5 μm. Line with squares, F(y) for light with polarization orthogonal to YZ plane; Line with crosses, F(y) for light with polarization parallel to YZ plane; Line with rhombs, F(y) for nonpolarized light.

expressions for the Fresnel coefficients) and then numerically integrated using Simpsons rule. The contributions for the different values of ϕ are transformed back to the original XYZ coordinates and then numerically integrated, again using Simpsons rule. The number of different values for θ and ϕ is taken in such a way that the total error in F_Z and F_Y is less than 0.5%. Typical results are shown in Figures 3–5.

Figure 3 shows the force in the direction of the incident light as a function of the distance between the focus and the center of the sphere for a number of relative refractive indices; the sphere has a diameter of 7.5 μm and the focus has a radius of 1.8 μm. The dip in the magnitude of F_Z after the focus is caused by the nearly orthogonal incidence of the light rays at the focus: the reflection force is low near orthogonal incidence and the refraction force has a low z component near orthogonal incidence. For very low refractive indices the force becomes negative (that is in the direction of the focus) after the focus. The sphere acts as a weak positive lens and the refracted beam will be less divergent so that there is an increase in momentum in the z direction which is compensated for by a negative force on the sphere. The reflection forces, to a first approximation, yield a positive force but because the reflection for low relative refractive indices is smaller than the transmission, the force can be negative.

Figure 4 shows the force in the direction of the incident light as a function of the distance of the sphere to the focus for a glass sphere with a radius of 5 μm in a strongly divergent laser beam (radius of the focus is 0.29 μm). The force F_Z is negative shortly after the focus. This was experimentally observed by Ashkin (5) but not yet theoretically calculated.

Figure 5 shows the differences in F_Y (positive in the direction of the beam axis) as a function of the distance y from the beam axis for different polarizations of the incoming light. The differences can be explained by the fact that, if the sphere is somewhat off the beam axis in the y direction, light with a polarization orthogonal to the YZ plane is mainly scattered with its polarization orthogonal to the plane of reflection; the reflection coefficient has a higher value at this polarization and the reflection forces are therefore higher than for incident light with the polarization parallel to the YZ plane.

EXPERIMENTAL SET-UP AND MEASURING METHODS

To test some of the predictions of the geometrical optics model we measured the radiation forces on two different kinds of dielectric spheres with diameters of 7.5 and 32 μm in a gravity trap. Schematic drawings of the configuration used are shown in Figure 6A and 6B.

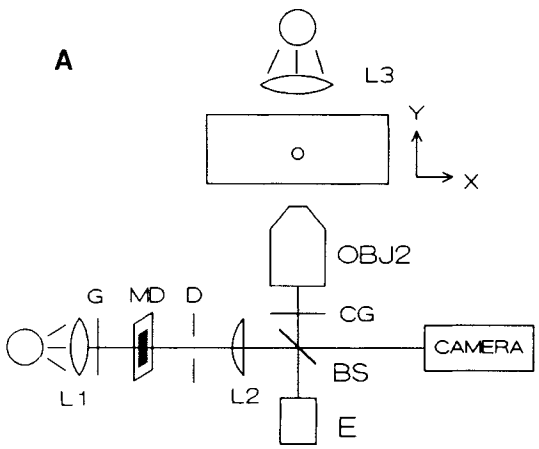

FIG. 6A. Schematic drawing of the configuration used: measuring system (seen from above). L, lens; OBJ, objective; G, ground glass; MD, millimeter division; D, diaphragm; BS, beam splitter; CG, color glass; E, eyepiece.

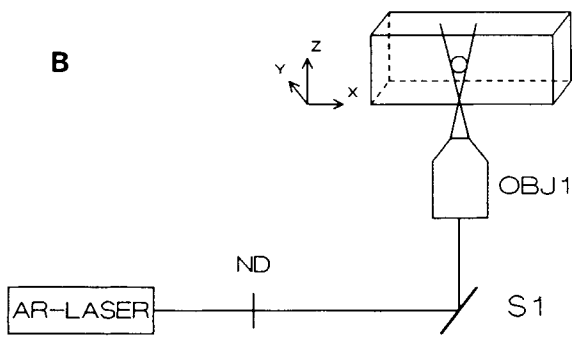

FIG. 6B. Schematic drawing of the configuration used: gravity trap (seen from aside); the cuvet can be moved in X, Y, and Z direction. AR-Laser, Argon laser (λ = 488 nm); ND, neutral density filter; S1, mirror; OBJ, objective.

Light from a 0.1 W Argon laser (model 5500 AWC, Ion Laser Technology, Salt Lake City, UT) with λ = 488 nm, polarized parallel to x axis, was focused to a spot with a radius of 1.79 μm using a Leitz 32/0,40 objective (Leitz Gmbh, Wetzlar, West Germany). The spheres were suspended in distilled water and contained in a quartz cuvet (Hellma GMBH, West Germany). The cuvet can be moved in X, Y, and Z direction using three encoder stepper mikes and an encoder mike controller (model 18011, Oriel Corporation, Stratford, CT).

The position of the spheres inside the cuvet was monitored with a Panasonic F10 ccd camera (Matsushita Electrics, Japan); at the same time a millimeter division was projected so that the position of the spheres relative to the focus could be measured. Measurements were recorded using a S-VHS video recorder (JVC HR-S5000E). The millimeter division was calibrated in two ways, first using a microscope calibration target and second using the stepper mikes (resolution < 0.5 μm); both calibrations were in excellent agreement. The power of the laser light inside the cuvet was calculated by measuring at points in front of and behind the cuvet with a power monitor (Scientech 361-2229, Scientech, Inc, Boulder Colorado, CO) and correcting for the losses at the transitions.

Two kinds of spheres were used, blank spheres (material unknown) of 7.5 μm diameter (mean), refractive index of 1.54 $\pm$ 0.02, and specific gravity of (1.197 $\pm$ 0.002) $\times$ 10^3 kg/m^3 (Flow Standards Corporation, Research Triangle Park NC) an blank polystyrene spheres of 27.4 μm diameter (mean), refractive index of 1.60, and specific gravity of 1.0495 $\times$ 10^3 kg/m^3 (Polysciences, Inc., Warrington PA).

For the 7.5 μm spheres the refractive index and specific gravity had to be measured, for the 27.4 μm spheres the refractive index was taken from the handbook of Chemistry and Physics (ed. 57), the specific gravity was measured. The refractive index was measured by comparing it to the refractive indices of fluids with known refractive indices. The specific gravity was measured using a sucrose gradient.

In the static method, F_Z was measured by determining the equilibrium positions in the gravity trap as a function of the power "p" of the incident light: $F_z(p) = F_G$ and then calculating the value of F_Z at a power of 1 W: $F_Z(1) = F_Z(p)/p$. This method is limited to the regions where $\partial F_Z(z)/\partial z < 0$, since only there we can have an equilibrium. The maximum possible error in the measurement of F_Z, using the static method, is estimated to be 10%. F_Z can also be measured in the unstable regions by continuous measurement of z and coupling this information back to the laser as done by Ashkin (2). We developed a more simple dynamic method by measuring the velocity v of a sphere under the influence of the forces F_Z and F_G. One finds:

$$m \cdot a = \Sigma F = F_z(z) - F_g - 6\pi\eta r v(z),$$

where $6\pi\eta rv$ is the Stokes force caused by friction (η is the viscosity of water). One can show that Σ F is always very small compared to the three forces individually if the acceleration of the particle is not more than 1 mm/s; in that case the velocity is continuously determined by F_Z:

$$F_z(z) = 6\pi\eta r v(z) - F_g.$$

If one makes $F_Z > F_G$ for all positions along the beam axis, one can determine v(z) by measuring z as a function of time and calculate $F_z(z)$. The velocity v(z) was measured using the still picture option of the video recorder (25 pictures per s). The maximum possible error in the measurement of F_Z, using the dynamic method, is estimated to be 30%.

EXPERIMENTAL RESULTS

Typical results of force measurements for dielectric spheres of 7.5 μm and a refractive index of 1.54 are shown in Figure 7. The crosses represent the static

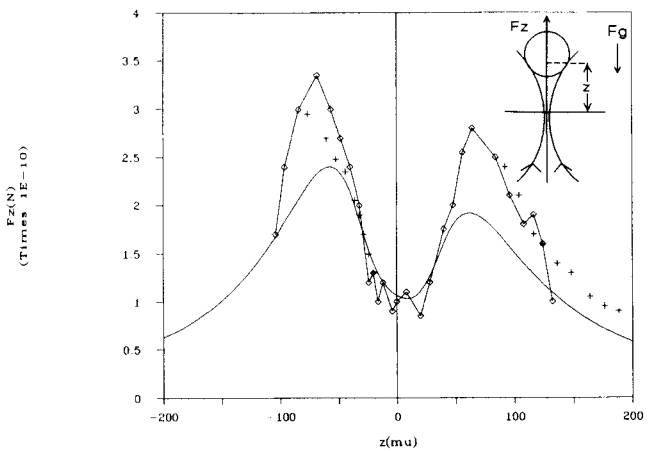

FIG. 7. Measurements of f(z) as a function of z relative to the calculated values for spheres with a radius of 3.75 μm and a focus with a radius of 1.8 μm. Solid line, calculated values for a refractive index of the sphere = 1.54. Line with rhombs, dynamic measurements. Crosses, statical measurements.

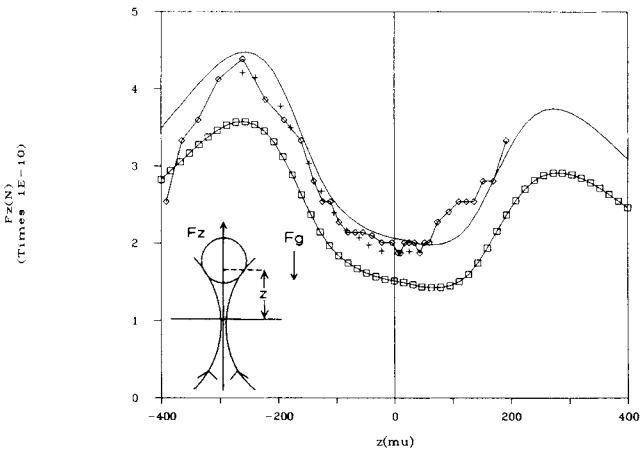

FIG. 8. Measurements of f(z) as a function of z relative to the calculated values for spheres with a radius of 16 μm and a focus with a radius of 1.8 μm. Solid line with squares, calculated values for a refractive index of the sphere = 1.60. Solid line, calculated values for refractive index of the sphere = 1.65. Line with rhombs, dynamic measurements. Crosses, statical measurements.

measurements and the line with rhombs represents the dynamic measurements. The solid line represents the geometrical optics prediction calculated for the experimental conditions.

Figure 8 shows the measurements for dielectric spheres of 32 μm and a refractive index of about 1.60. The crosses represent the statical measurements and the line with rhombs represents the dynamic measurements. The solid line with the white squares represents the calculated values using a refractive index of 1.60; the solid line represents the geometrical optics prediction calculated for the experimental conditions and a refractive index of 1.65.

DISCUSSION

The numerical results of our model show a qualitative agreement with all measurements done. The model is also able to explain the observations of Ashkin of a single beam optical trap. The calculated values for the single beam gradient force optical trap are also in agreement with the experimental results of Ashkin; at a laser power of 100 mW one finds a maximum attractive force of 2.5×10^{-12} N which is greater than the gravity force on a 10 μm glass sphere ($F_g \cong 7.5 \times 10^{-13}$ N).

The measured values show a good qualitative correlation with the numerical results as can be seen from Figures 7 and 8. For the spheres of 7.5 μm there seem to be small differences in the positions of the maxima and minima. This might be due to the fact that these spheres are too small to justify the use of the geometrical optics model. For spheres with a diameter of 7.5 μm the value of $2\pi\rho/\lambda$ is 64 which is somewhat lower than a value 100 required for the geometrical optics approach. For the spheres with a diameter of 32 μm the value of $2\pi\rho/\lambda$ is 275 which justifies the use of the geometrical optics model.

The qualitatively good correlation between the numerical and experimental results show that the model can be used to predict the stability of an optical trap for spheres with a diameter of 7.5 μm or larger. The stability is determined by the negative slopes in the graphs (the steeper the slope, the more stable the trap).

The static and dynamic measurements show a very good agreement. For both kinds of spheres the measured values are somewhat higher as the calculated values; measurements for F_Y (not shown here) show the same effects. The difference in the calculated and measured values might be due to systematic errors in our measurements, to systematic errors in our calculations, to wrong assumptions in the model, or, in the case of the small spheres, it might be due to the fact that the model is not entirely valid.

Systematic errors in our measurements seem unlikely considering the differences between the calculated and the measured values of the different spheres. For the 7.5 μm spheres there is a very good agreement near the focus and the differences occur away from the focus. For the 32 μm spheres the differences between the calculated values for (n = 1.60) and the measured values are more uniform.

To verify our numerical calculations we reproduced the results of Roosen (12). Our calculations show excellent quantitative and qualitative agreement with the theoretical results of Roosen whose measurements of radiation pressure on large solid glass spheres are in quantitative agreement with the theoretical results he obtained.

The best possible explanation therefore is that we made wrong assumptions in the model or that the

model is not entirely valid. A possible explanation is that for small spheres resonance phenomena can occur (3,10). These resonances are thought to be caused by dielectric surface waves and should only appear when light hits the edge of the spheres. This is not true near the focus for the spheres we used (diameter of the sphere is greater than diameter of the beam waist) but only when $w_0 \geq r$; using (9) one calculates that this is true at a distance $z = 50$ μm from the focus, just where the differences between the measured and the calculated values occur (see Fig. 7). These resonances therefore gives a very plausible explanation for the differences between our calculated and measured values for the 7.5 μm spheres.

A second possibility is that the assumption that the spheres do not absorb is not completely correct. If the spheres partially absorb the used model is not correct and the resulting radiation forces will be higher than expected but will probably be in qualitative good agreement with the forces for non absorbing spheres because of the reflection and refraction part.

It should be noted that the magnitude of the calculated forces is very sensitive for the refractive index. For the 32 μm spheres we used a refractive index of 1.60, but when one assumes a refractive index of 1.65 [as done by Ashkin (5)] one gets a very good agreement between the theoretical and experimental results as can be seen in Figure 8.

In conclusion we believe that the geometrical optics model can be used to predict the regions where stable optical trapping is possible and that it can be used to predict the stability of an optical trap, even for spheres with a radius smaller than the value given by $2\pi\rho/\lambda \geq 100$.

LITERATURE CITED

1. Ashkin A: Acceleration and trapping of particles by radiation pressure. Phys Rev Lett 24:156–159, 1970.
2. Ashkin A: Feedback stabilization of optically levitated particles. Appl Phys Lett 30:202–204, 1977.
3. Ashkin A, Dziedzic JM: Observation of resonances in the radiation pressure on dielectric spheres. Phys Rev Lett 38:1351–1354, 1977.
4. Ashkin A, Dziedzic JM: Internal Cell manipulation using infrared laser traps. Proc Natl Acad Sci USA 86:7914–7918, 1989.
5. Ashkin A, Dziedzic JM, Bjorkholm JE, Chu S: Observation of a single beam gradient force optical trap for dielectric particles. Opt Lett. 11;288–290, 1986.
6. Block SM, Blair DF, Berg HC: Compliance of bacterial flagella measured with optical tweezers. Nature 338:514–518, 1989.
7. Brevik I: Experiments in phenomenological electrodynamics and the electromagnetic energy-momentum tensor. Phys Rep 52:133–201, 1979.
8. Buican TN, Smyth J, Crissmann HA, Salzman GC, Stewart C, Martin JC: Automated single-cell manipulation and sorting by light trapping. Appl Opt 26:5311–5316, 1987.
9. Hulst, HC v/d. Light scattering by small particles. Dover Publications, Inc, New York, 1957, pp 224–226.
10. Irvine WM: Light scattering by spherical particles: Radiation Pressure, Asymmetry factor, and extinction cross section. J Opt Soc Am 55:16–21, 1964.
11. Kogelnik H, Li T: Laser beams and resonators. Proc IEEE 54: 1312–1329, 1966.
12. Roosen G, Delaunay B, Imbert C: Étude de la pression de radiation exercée par un faisceau lumineux sur une sphère réfringente. J Opt (Paris) 8:181–187, 1977.